applied sciences

MDPI

Article

Introducing a Novel Application of Bio-Based Fillers Based on Rice Bran Wax Infused with Green Tea: Transitioning from a Cosmetic Additive to a Multifunctional Pigment for Wood Paints

Massimo Calovi * and Stefano Rossi

Department of Industrial Engineering, University of Trento, Via Sommarive 9, 38123 Trento, Italy; stefano.rossi@unitn.it

* Correspondence: massimo.calovi@unitn.it; Tel.: +39-04-6128-2403

Abstract: This study aims to assess the functionality of a bio-derived additive, comprising rice bran wax infused with green tea, as an environmentally sustainable and adaptable pigment for wood coatings. Additionally, the effectiveness of the bio-based additive, in conjunction with a specialized UV absorber to enhance color consistency under harsh conditions, was examined. Aesthetic impact was analyzed through evaluations of color, gloss, and surface roughness. Moreover, the stability of the wax-based powder in aggressive environments was characterized by subjecting samples to UV-B and climatic chamber exposure. The barrier properties of the additive were investigated using a water uptake test and contact angle measurements, while liquid resistance tests were conducted to gauge its efficacy. Lastly, the protective role of the bio-based additive was analyzed through scrub tests and surface analysis using scanning electron microscopy. Findings underscored the versatility of the *green* additive as a multifunctional pigment, offering not only color enhancement but also robust protective capabilities. Its unique combination of color, mattifying effect, barrier enhancement, and protective function position it as an attractive bio-based additive for wood coatings with functional applications.

Keywords: rice bran wax; green tea; UV absorber; bio-based filler; wood paint; coating durability

Citation: Calovi, M.; Rossi, S. Introducing a Novel Application of Bio-Based Fillers Based on Rice Bran Wax Infused with Green Tea: Transitioning from a Cosmetic Additive to a Multifunctional Pigment for Wood Paints. *Appl. Sci.* **2024**, *14*, 5895. https://doi.org/10.3390/app14135895

Academic Editors: Irene Gouvinhas and Juliana Garcia

Received: 12 June 2024
Revised: 28 June 2024
Accepted: 3 July 2024
Published: 5 July 2024

1. Introduction

The wood coatings industry is currently prioritizing the tenets of the closed-loop economy, focusing on reducing waste by utilizing natural resources and repurposing materials that were once considered industrial waste [1]. Recent research highlights significant efforts by both researchers and industry professionals to develop innovative, eco-friendly wood protection methods using advanced technologies and sustainable materials [2]. This involves exploring bio-based organic matrices for environmentally friendly protective coatings, incorporating sustainable fillers and additives, and utilizing the properties of natural pigments and dyes [3].

Vegetable oils and their derivatives are emerging as promising alternatives for coating matrices, potentially replacing conventional polymeric ones [4]. These oils offer additional benefits such as antibacterial and antifungal properties [5,6], hydrophobic characteristics [7], self-cleaning abilities [8], and UV protection [9]. Similarly, natural biopolymers like chitosan, alginate, and cellulose are viable options [10]. The preservatives and impregnators industry is also shifting towards bio-based materials sourced from plants [11–13] and vegetables [14–16] to combat harmful fungi affecting wood [17–19].

A key area of interest is the use of bio-based fillers and protective additives in wood coatings, which can be customized to enhance weather resistance, as seen with materials

like hemp-based biocarbon [20], lignin [21], and tannin [22]. These additives also strengthen eco-friendly coatings, with cellulose derivatives showing strong potential [23–25]. Additionally, many natural fillers have notable antimicrobial properties, including extracts from coffee [26], propolis [27], and essential oils [28]. Another growing focus is the use of alternative and eco-friendly pigments and dyes. The wood paint industry is increasingly creating coatings with vibrant colors [29] for unique and appealing aesthetics [30,31]. For example, the coloring potential of natural pigments from sources like spirulina [32,33], turmeric [34], and wood waste [35] is being explored, along with microbial pigments [36,37] that offer greater functionality and sustainability compared to traditional methods.

Given these considerations, this study seeks to assess the application of a composite additive for wood paints, characterized as bio-based, which integrates both protective and aesthetic attributes. This additive consists of ultrafine rice bran wax powder infused with green tea.

Previous research has explored the functional properties of rice bran wax powders as bio-based fillers for wood coatings, revealing their outstanding effectiveness in improving the surface's hydrophobic properties and reinforcing the coatings' mechanical durability [34]. Rice bran wax qualifies as a *green* additive since it is a natural wax derived from the husk or bran of rice (*Oryza sativa*), a by-product of rice production. Rice bran is extensively grown and processed globally as a major food crop [38]. The wax is extracted during the refining of rice bran oil [39,40] through a dewaxing process that encompasses phases such as gum removal, acid reduction, color stripping, odor elimination, and cold stabilization [40,41]. Owing to its inherent hydrophobic properties, rice bran wax appears to be a plentiful and economical bio-based filler, augmenting the protective capabilities of organic coatings. Recent research indicates that the low surface free energy of wax [42,43] can markedly improve the hydrophobic characteristics of wood [44]. Green tea, on the other hand, is sourced from the leaves of *Camellia sinensis*, a species in the *Theaceae* family. It is grown in no fewer than 30 nations worldwide [45]. Because of its unique hue, antimicrobial properties, and antioxidant activity, green tea extracts are commonly used in skincare and cosmetic products [46–48].

Consequently, the company Micro Powders (Tarrytown, NY, USA) has combined the two bio-based materials, namely rice bran wax and green tea extracts, to develop a powder specifically designed for color cosmetics applications, called *Naturesoft® 880GT*.

Thus, this study assesses the efficacy of this *green* additive in enhancing the properties of wood coatings, while also considering the aesthetic enhancements introduced by the tea extract. However, due to the potential for the natural green color of the product to fade when exposed to light, the research also involves applying the filler in conjunction with a dedicated UV absorber, called *Uvasorb® S130*, to prolong the aesthetic durability of the *green* additive. This particular additive has been subject to extensive research as a protective element in both organic [49,50] and hybrid [51] coatings, frequently in combination with amine light stabilizers [52]. Furthermore, its effectiveness as a protective agent for wood coatings has been previously validated [53]. Ultimately, the objective of the study is to underscore the potential applicability of *green* additives, originally intended for other applications, as viable bio-based reinforcing and coloring materials, aligning with the environmentally conscious principles of the wood paint sector. This study shows that rice wax is not merely an industrial byproduct but a versatile additive with the potential to enhance the protective qualities of organic wood coatings. Furthermore, incorporating green tea into the wax adds aesthetic appeal, transforming it into an effective high-performance pigment.

2. Materials and Methods

2.1. Materials

The composite filler *Naturesoft®* 880GT, provided by Micro Powders (Tarrytown, NY, USA), was used in its original form. The additive is a powder with a sage green hue, derived from *Oryza sativa* (rice) bran wax combined with *Camellia sinensis* leaf extract. Its

granules are irregularly shaped and typically range in size from 6.0 to 10.0 μm, with a density of 0.96 g/cc and a melting point ranging from 82 to 86 °C. *Uvasorb® S130*, supplied by 3V Sigma (Bergamo, Italy), was used as received. This liquid UV absorber, which ranges in color from yellow to brownish, consists of β-[3-(2-H-Benzotriazole-2-yl)-4-hydroxy-5-tert-butylphenyl]-propionic acid-poly(ethylene glycol) 300-ester + Bis[β-[3-(2-H-Benzotriazole-2-yl)-4-hydroxy-5-tert-butylphenyl]-propionic acid]-poly(ethylene glycol) 300-ester. The additive has a boiling point of 166 °C and a density of 1.17 g/cc. Poplar wood panels, sized 150 × 150 × 2 mm^3, were acquired from Cimadom Legnami (Lavis, TN, Italy). These panels exhibit a density ranging from 0.40 to 0.42 g/cm^3 and a moisture content varying between 6% and 9%. Poplar plywood, selected as the substrate for applying paint, is esteemed for its superior quality compared to other panel materials [54]. Its exceptionally sleek surface makes it suitable for painting, laminating, or veneering [55]. Additionally, its remarkable ease of fabrication, notably its reputation for effortless cutting, sanding, or screwing, positions it as the preferred material for creating diverse samples intended for a broad range of characterization tests. Lastly, the water-based acrylic paint, named *TECH20*, was provided by ICA Group (Civitanova Marche, AN, Italy). Formulated from materials obtained from sustainable and renewable sources, this paint has a density ranging from 1.01 to 1.18 g/mL and a viscosity of 50 to 60 s as measured by the Ford Viscosity Cup 5.

2.2. Samples Fabrication

The production of samples started with the poplar wood panels undergoing initial preparation using 320 grit abrasive paper to eliminate any exposed fibers and achieve a notably polished surface, enhancing the adherence of the coating and preventing the formation of imperfections. Subsequently, the coatings were applied through spray application, following the instructions provided by the manufacturer. Specifically, a material rate of 100 g/m^2 was applied under a pressure of 3 bar.

The research encompasses the characterization of four distinct series of samples, the compositions of which are outlined in Table 1. Two varying amounts of the bio-based additive were incorporated into the clear paint to assess their effects on aesthetics and functionality, particularly focusing on barrier and abrasion resistance properties. Specifically, concentrations of 5 wt.% and 10 wt.% were examined and selected based on preliminary tests to achieve the desired color in the coating. Consequently, samples G5 and G10 were produced, respectively. Given the manufacturer's caution regarding potential color degradation of the bio-based filler upon light exposure, sample G10U incorporated not only 10 wt.% of *Naturesoft® 880GT* but also 3 wt.% of UV absorber *Uvasorb® S130*. The amount of UV absorber was determined based on preliminary tests performed in previous literature studies [56]. Ultimately, the effectiveness of these three groups of composite coatings was evaluated in comparison to the behavior exhibited by sample G0, which utilized transparent acrylic paint without any additives. This sample G0 thus acts as a reference point, aiding in the better understanding and evaluation of the contributions provided by the bio-based filler and the UV absorber.

Table 1. Composition of samples with corresponding nomenclature.

Samples Nomenclature	Additives Incorporated into the Paint Formulation
G0	/
G5	5 wt.% *Naturesoft® 880GT*
G10	10 wt.% *Naturesoft® 880GT*
G10U	10 wt.% *Naturesoft® 880GT* + 3 wt.% *Uvasorb® S130*

To achieve consistent dispersion of the different additives within the paint, each solution underwent mechanical blending for 30 min prior to application on the wooden sub-

strate. This mixing process ensured a uniform distribution of the components in the solution, preventing any instances of settling or uneven distribution. The coating production involved spraying the first layer and allowing it to cure at room temperature for 4 h. Following this, a second layer was applied to achieve a final compact coating with a thickness of approximately 100 μm.

2.3. Characterization

Initially, the morphology of the bio-based additive derived from rice bran wax was examined using a low vacuum scanning electron microscope (SEM JEOL IT 300, JEOL, Akishima, Tokyo, Japan). The analyses were conducted using an acceleration voltage of 15.0 kV and operating at a working distance (WD) of 10.0 mm. Furthermore, energy-dispersive X-ray spectroscopy (EDXS, Bruker, Billerica, MA, USA) was employed to analyze its chemical composition. Additionally, SEM was employed to examine cross-sections of the coatings, offering insights into how various additives and their concentrations impact the structure of the composite layers. To assess the visual characteristics of the coatings and illustrate the influence of additives on their overall appearance, colorimetric analyses were conducted using a Konica Minolta CM-2600d spectrophotometer (Konica Minolta, Tokyo, Japan) with a D65/10° illuminant/observer configuration in SCI mode. Gloss measurements following the ASTM D523/14 standard [57] were performed using an Erichsen 503 instrument from Erichsen Co.Fo.Me.Gra Instruments (Milan, Italy). A total of 9 assessments of color and gloss were performed on 3 samples per series, with 3 measurements per sample. Furthermore, the aesthetic influence of the additives was evaluated through surface texture analyses of the coatings using the MarSurf PS1 mobile surface roughness measurement device (Carl Mahr Holding, Göttingen, Germany).

To assess the long-term aesthetic performance of the bio-based additive under harsh conditions and the protective efficacy of the UV absorber, samples underwent accelerated degradation tests in a UV chamber for 48 h. The UV chamber used was a UV173 Box Co.Fo.Me.Gra (Co.Fo.Me.Gra, Milan, Italy), following ASTM D4587-11 standard procedures [58]. This includes exposure to UV-B radiation (313 nm) at 60 °C. During the exposure period, colorimetric and gloss analyses were conducted to assess the coatings' visual uniformity and investigate the influence of various additives.

Likewise, the heat resistance of the paint was tested by analyzing the color and gloss changes in the samples exposed to severe thermal variations simulated using the climatic chamber ACS DM340 (Angelantoni Test Technologies, Perugia, Italy). The exposure test followed the UNI 9429 standard [59] and involved 15 cycles, each consisting of:

- 4 h at +50 °C and relative humidity below 30%;
- 4 h at −20 °C;
- 16 h at room temperature.

To prevent moisture absorption by the poplar wood substrate, silicone was applied to seal the five untreated sides of the 40 × 40 × 2 mm^3 samples. This sealing procedure was conducted before the experiments to maintain the integrity of the wood substrate.

The impact of additives on the barrier properties of the coatings was initially evaluated using a liquid water absorption test, conducted following the EN 927-5:2007 standard [60]. Five uncoated surfaces of 40 × 40 × 2 mm^3 poplar wood panels were effectively sealed with silicone to prevent water absorption into the wood substrate. Prior to testing, the samples were conditioned at 65% relative humidity and 20 °C. They were subsequently immersed in a container filled with water, and the amount of moisture absorbed, measured in grams per square meter (g/m^2), was recorded at intervals of 6, 24, 48, 72, and 96 h. Three samples per series were included in the test. Additionally, the visual appearance of the samples was tracked during the test using colorimetric measurements and gloss analysis.

In a similar manner, the test for resistance to cold liquids was performed to assess how well the coatings could endure exposure to different chemical substances, in accordance with the UNI EN 12,720 standard [61]. For this examination, filter paper (weighing 90 g/m²) was immersed in separate solutions containing 15% sodium chloride, pure acetone, olive oil, and coffee. Additionally, the coatings' ability to resist acidic and alkaline conditions was evaluated using solutions adjusted to pH levels of 1 and 14, respectively, achieved with concentrated hydrochloric acid (HCl) and sodium hydroxide (NaOH). These soaked filter papers were placed on the coating surface under a glass cover for a 24 h duration. Subsequently, the glass cover and filter paper were removed, and any residual liquid on the coating surface was meticulously wiped off. Color and gloss assessments were carried out concurrently with both the liquid water absorption test and the cold liquid resistance test to evaluate the coatings' aesthetic uniformity.

In conjunction with these examinations, contact angle assessments were executed according to the ASTM D7334-08 standard [62] to analyze how different additives affect the coating's ability to repel water. Large-scale images were taken using a Nikon 60 mm lens with an aperture set to f/2.8 (Nikon Instruments Europe, Amstelveen, The Netherlands). Contact angle measurements were performed using the NIS-Elements Microscope Imaging software, specifically Windows Version 4.30.01. Droplets of demineralized water (5 μL) were dispensed from a syringe, released from 2 cm above the surface. After resting on the coating for 60 s, each droplet was captured in a photograph, and the wetting angle was determined using the imaging software. To ensure statistical validity, 3 samples per series underwent 5 measurements each, facilitating a thorough analysis of the coating's surface wettability traits.

Finally, the protective capability of the bio-based filler regarding abrasion resistance was examined using the scrub test. This experiment involved testing 5 samples per series (measuring 150 × 80 × 2 mm³) using an Elcometer 1720 Abrasion and Washability Tester (Elcometer, Manchester, UK), following the ISO 11,998 standard [63]. The test utilized the standardized sponge Tool 5 weighing 232 g. Importantly, unlike the conventional procedure, this test was conducted dry, without the use of a cleaning solution. This modification aimed to prevent the solution from penetrating the polymeric matrix and wood, potentially influencing the results. Mass loss from the coatings was monitored after 250, 750, 1500, and 3000 cycles, with a frequency of 37 cycles per minute. Furthermore, the impact of the abrasive test on the coating's aesthetic properties was evaluated through analysis of color, gloss, and roughness. Moreover, SEM observations were conducted at the conclusion of the test to evaluate the impact of the abrasive sponge on the morphology of the samples, specifically examining the role of the bio-based additive in mitigating the abrasive process.

3. Results and Discussion

3.1. Filler and Coatings Aspect

The structural morphology of the bio-based wax additive was initially examined using SEM, as shown in Figure 1. The analysis verified the information provided in its technical data sheet, revealing that the powder is composed of granules characterized by an irregular shape, with an average size of approximately 10 μm. This size is well-suited for applications like additives and fillers in paints and organic coatings, where typical thicknesses range in the order of tens of μm. The EDXS analyses, depicted in Figure A1 of the Appendix A, demonstrate the organic composition of the wax-based additive, primarily consisting of carbon and oxygen. This suggests that the filler is devoid of any inorganic elements or contaminants that might affect its performance.

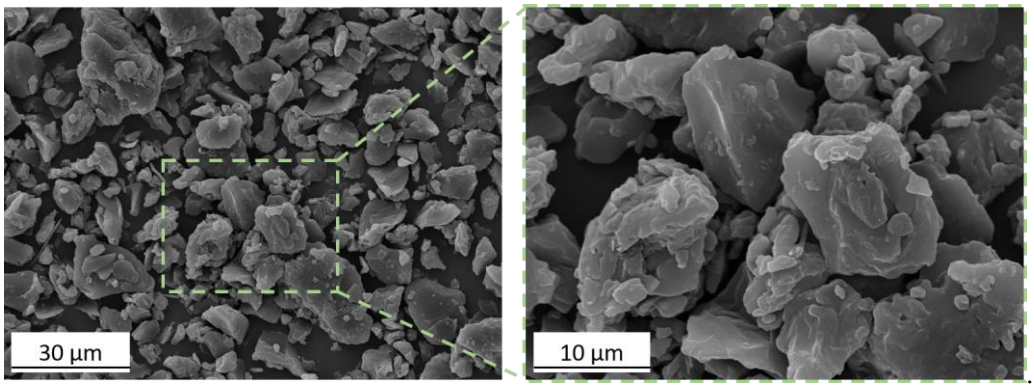

Figure 1. SEM micrograph of the bio-based filler, acquired in secondary electrons mode.

Thus, the additive was incorporated into the acrylic paint formulation to produce the four series of samples detailed in Table 1, with their appearances illustrated in Figure 2a. The additive exhibits a significant coloring effect, notably altering the appearance of the coating to green–yellow hues. This visual effect becomes more pronounced with increasing additive concentration, evident from the transition from sample G0, which is transparent, to samples G5 and G10, containing 5 wt.% and 10 wt.% of wax, respectively. Simultaneously, the UV absorber included in sample G10U does not counterbalance the chromatic effect of the green tea-infused wax, as samples G10 and G10U exhibit identical appearances. However, to quantify and qualify the aesthetic distinctions among the four series of samples, they underwent colorimetric measurements. Figure 2b displays the values of the three color coordinates L*, a*, and b*. In colorimetry, these coordinates represent specific color attributes, where:

- L* represents lightness, varying from 0 (for black objects) to 100 (for white objects);
- The a* axis represents the red–green axis, with positive values indicating redness and negative values indicating greenness;
- The b* axis represents the yellow–blue axis, where positive values indicate a tendency towards yellowness and negative values indicate a tendency towards blueness.

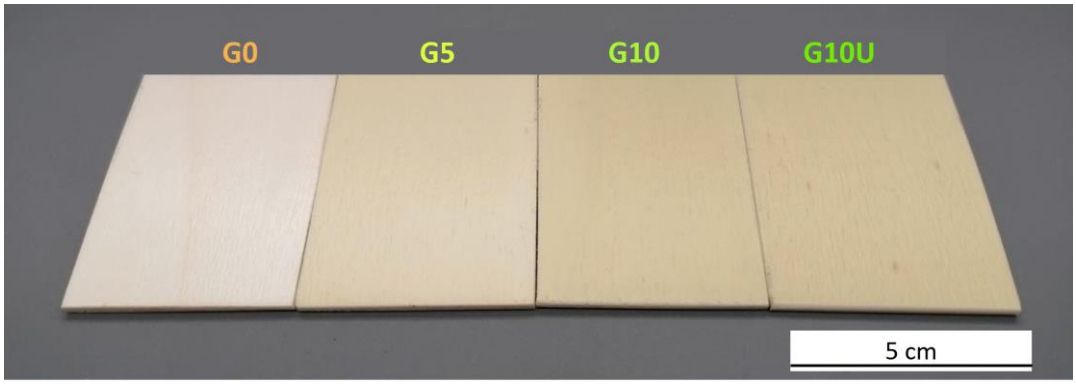

(**a**)

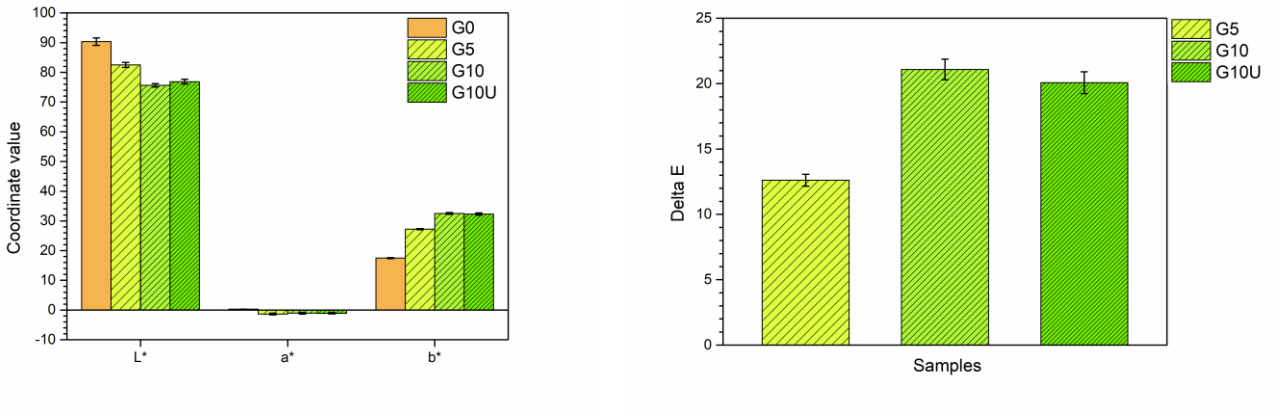

(**b**) (**c**)

Figure 2. (**a**) Visual appearance of the samples, (**b**) respective values of the three CIE Lab coordinates, and (**c**) variations in color ΔE relative to the reference sample G0.

The inclusion of the *green* additive results in a decrease in the L* coordinate, indicating slightly darker shades. Additionally, as the additive concentration increases, the value of the b* coordinate rises towards yellower shades. As visually observed in Figure 2a, the simultaneous presence of the UV absorber in sample G10U does not yield any aesthetic impact, as evidenced by the negligible alteration in the values of the three coordinates compared to sample G10. To emphasize the chromatic influence of the bio-based additive, the color change ΔE compared to sample G0 was evaluated, and calculated according to the formula [64]:

$$\Delta E = [(\Delta L^*)^2 + (\Delta a^*)^2 + (\Delta b^*)^2]^{1/2} \quad (1)$$

The values of ΔE for the three series of composite coatings are depicted in the graph of Figure 2c. There is an almost proportional relationship between the additive concentration and the chromatic alteration of the coating, with ΔE values nearly doubling as the wax powder infused with tea increases from 5 wt.% to 10 wt.%. Indeed, sample G5 exhibits a color change compared to the reference sample G0 of approximately 12 units, whereas samples G10 and G10U show a ΔE of approximately 20–21 points. These color change values can be deemed substantial, particularly in light of the literature considerations, which define color changes of 1 unit as appreciable even to the human eye [65]. The error bars in Figure 2b,c are narrow, indicating the high reproducibility of the colorimetry measurements conducted.

However, the wax-based additive also affects the texture of the coating, in addition to its color. The bio-based powder leads to an important reduction in gloss values, as illustrated in the graph in Figure 3a, indicating a pronounced opacity of the coating. Indeed, even a 5 wt.% addition of the powder is sufficient to reduce the gloss values of the paint from 50 to 20. This reduction is further pronounced, albeit not linearly, by doubling the quantity of *green* additive. Once again, the UV absorber demonstrates no impact on the aesthetics of the coating, without influencing the behavior of the wax-based filler. However, as reflectance values of a surface are often closely linked to its roughness values, the samples underwent surface roughness measurements to discern whether the varied gloss values are attributed solely to the presence of wax or to different surface textures. Figure 3b exhibits the results of these analyses. Considering that paint tends to conform to the surface morphology of the substrate upon which it is applied, the measurements were carried out both parallel (Ra//) and perpendicular (Ra⊥) to the fibers of the wooden substrate, anticipating distinctly different outcomes. Indeed, the Ra⊥ values are significantly higher than those of Ra//, mainly due to the influence of the wooden panel's morphology. However, simultaneously, all four series of samples display roughness values that are

comparable to each other, indicating that the bio-based additive does not impact the surface morphology of the composite layer. This finding further confirms that the variations in gloss values shown in Figure 3a are not a result of differing roughness in the coatings but are solely attributed to the presence of the wax-based additive, which demonstrates noticeable matting capability. Similarly, analogous behaviors have been previously observed in the literature concerning wax-based fillers [32,34].

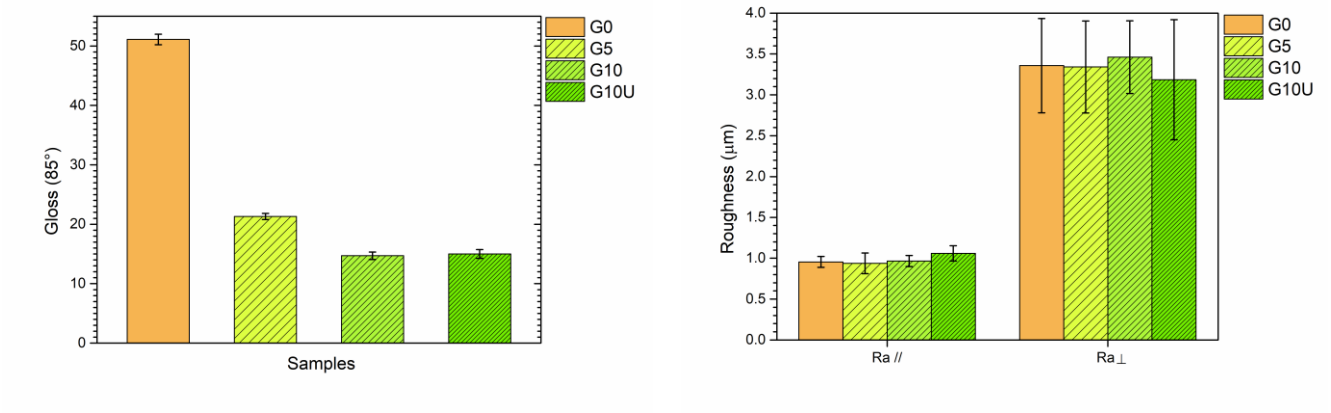

(**a**) (**b**)

Figure 3. (**a**) Gloss measurements of the four series of samples and (**b**) surface roughness of the coatings in parallel (Ra//) and perpendicular (Ra⊥) orientations.

Ultimately, the influence of the additives on the structure of the coating was assessed by examining the cross-section of the samples under SEM, following a brittle fracture process carried out in liquid nitrogen. The images in Figure 4 illustrate an example of the internal structure with a cross-section view of the four sets of samples, emphasizing the bulk morphology of the coating. As previously described, the coatings in the four sets of samples have comparable thicknesses, approximately 100 µm. Consequently, both the wax powder and the UV absorber additives do not influence the deposition process or alter the rheological properties of the paint. On the other hand, the SEM observations highlight that the addition of the wax-based powder produces a progressive structural modification of the layer, where the bulk appears significantly more intricate due to the presence of various extraneous bodies such as the granules of the *green* additive. Sample G10 in Figure 4c, in fact, demonstrates how the brittle fracture process leads to the release of many of these granules, resulting in a fracture surface that is not linear, akin to sample G0 (Figure 4a), but notably jagged. This phenomenon underscores and emphasizes that substantial amounts of additives can notably modify the internal structure of the coating. This aspect can be critical in some cases, leading, for example, to enhanced absorption of aggressive ions and diminished barrier properties of the composite layer due to a weak interface between the matrix and additive. Consequently, these features will be duly considered in subsequent tests pertaining to the barrier performance of the four series of coatings.

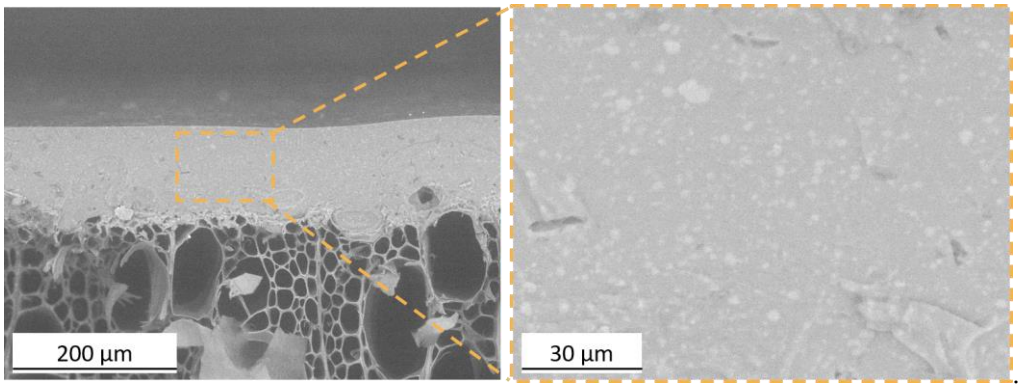

(**a**)

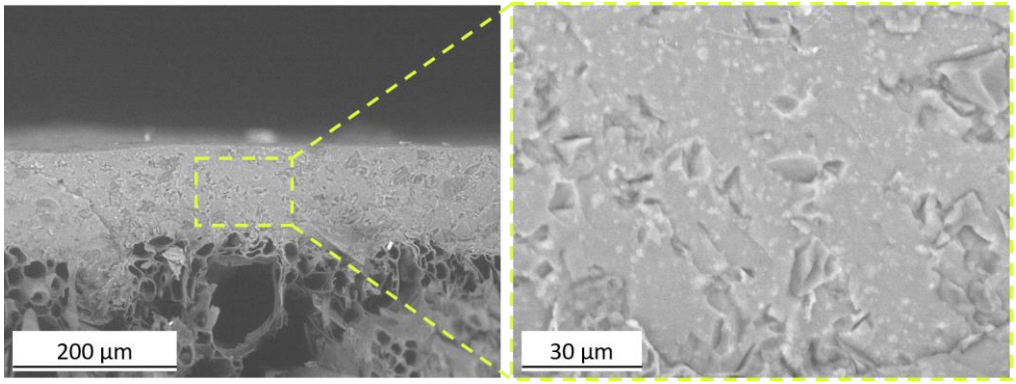

(**b**)

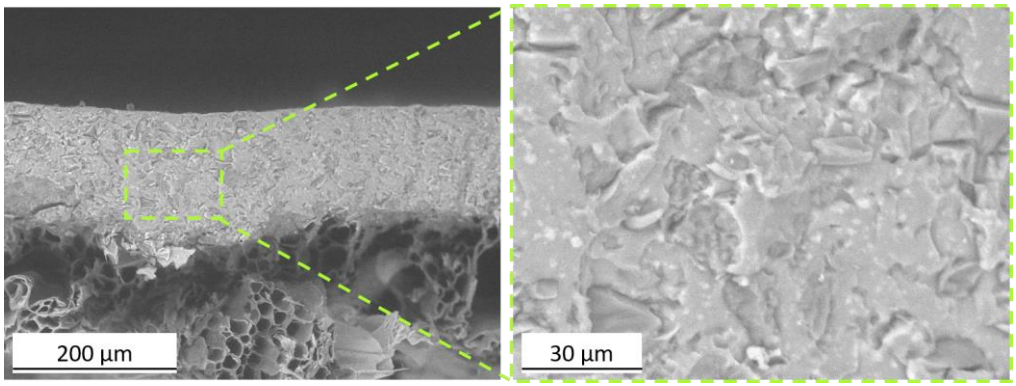

(**c**)

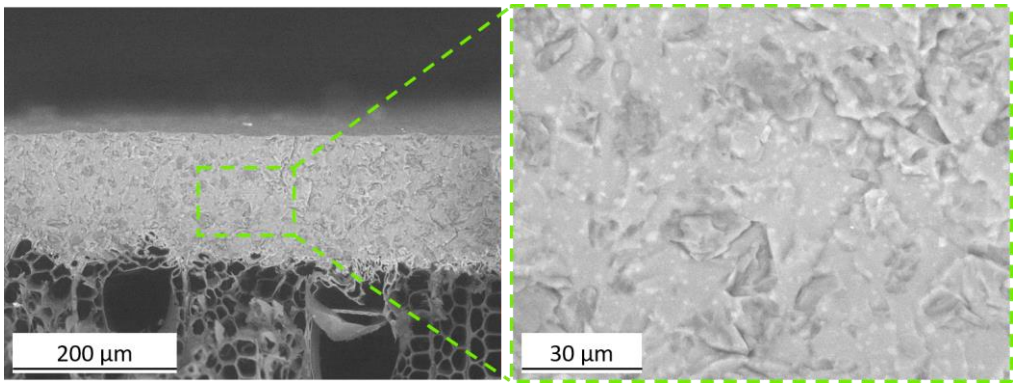

(**d**)

Figure 4. SEM micrographs of the cross-section of (**a**) sample G0, (**b**) sample G5, (**c**) sample G10, and (**d**) sample G10U.

In conclusion, the bio-based additive demonstrates commendable coloring power, thereby serving as an eco-sustainable pigment. Additionally, while not affecting the surface morphology of the coating, the wax component of the additive imparts a significant matting effect, which substantially alters the aesthetics and reflectance of the paint. Moreover, the additive appears to markedly modify the structure of the composite layer, necessitating thorough analyses of the barrier properties of the final coating upon its application. Lastly, the UV absorber appears to have no discernible influence on the aesthetic characteristics of the coatings, making it suitable for use as a functional additive without compromising the coloring properties of the tea-infused wax powders.

3.2. Aesthetic Durability of the Additive in Challenging Environments

Because tea extract's color durability is sensitive to outdoor environmental factors [66,67], the samples underwent characterization tests in harsh conditions. Figure 5 illustrates the observable aesthetic alterations of the coatings after exposure to UV-B radiation. Figure 5a depicts the progression of gloss values throughout the test, while Figure 5b accentuates alterations in color. Additionally, both graphs feature curves representing the untreated wood substrate, serving as a benchmark material for comparison. The narrow error bars once again affirm the reproducibility of both the gloss and colorimetry measurements conducted. Exposing the samples to a UV-B chamber results in noticeable aesthetic alterations. The reflectance properties of pure acrylic paint tend to diminish, as demonstrated by the gloss curve of the G0 sample. This behavior, consistent with previous research [68,69], is attributed to photodecay phenomena affecting the resin. Conversely, the samples incorporating the bio-based additive exhibit minimal changes in texture, as the wax promptly imparts opaque characteristics onto the composite coating. Furthermore, all four series of coatings, along with the wood substrate, exhibit a distinct color change represented by ΔE (Figure 5b). Poplar wood, in particular, demonstrates significant color alteration, attributed to photooxidation processes and degradation of cellulose, hemicellulose, and lignin [70–72]. The gradual increase in ΔE values observed in sample G0 is attributed to a slight degradation of the wooden substrate [73], not entirely shielded by the transparent coating. This phenomenon has been previously documented in a study [74], highlighting the inability of paints to entirely mitigate photooxidation effects in wood, especially evident when the coating is transparent. Concurrently, samples containing the green additive display noticeable color changes, with the degree correlating to the concentration of wax-based powder. This indicates that UV-B radiation triggers aesthetic degradation of the bio-based additive. The extent of these chromatic variations is mitigated to some degree by the UV absorber in sample G10U, resulting in lower ΔE values compared to sample G10. However, it is important to note that the chromatic degradation in sample G10U is still significant, albeit reduced. The UV absorber's impact is notable during the initial hours of exposure; however, as the test progresses, its effectiveness diminishes due to the aggressive nature of the conditions, rendering the protective component ineffective.

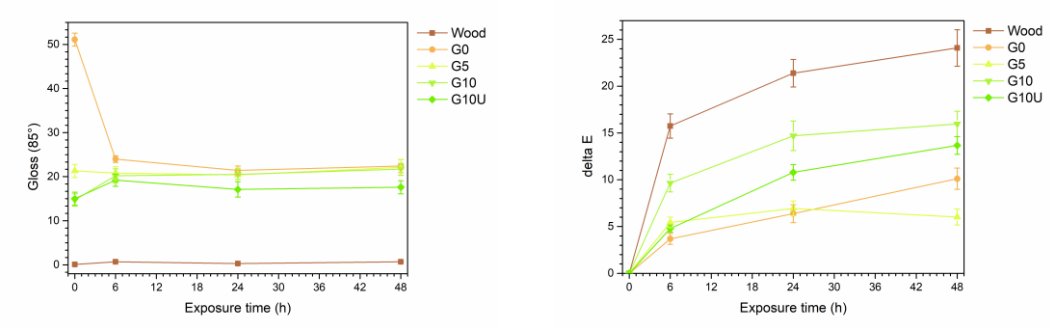

(**a**) (**b**)

Figure 5. Evolution of (**a**) gloss and (**b**) color during the UV-B chamber exposure test.

To underscore the deterioration of the wax-based additive infused with green tea, the same powder underwent the accelerated degradation test. Figure 6 illustrates the visual changes in the additive before (left) and after (right) 48 h of exposure in the UV-B chamber. The images clearly depict a significant transformation in the appearance of the additive, with the majority of the green–yellow component from the tea extract almost completely faded. Additionally, the temperature within the chamber (60 °C) causes partial melting of the wax-based powder. Indeed, while rice bran wax has previously shown resilience to UV-B radiation [34], various components of green tea are notably susceptible to decay. Green tea consists of 30–42% polyphenols [75], primarily catechins [76], which are particularly prone to degradation when exposed to light and temperature [77].

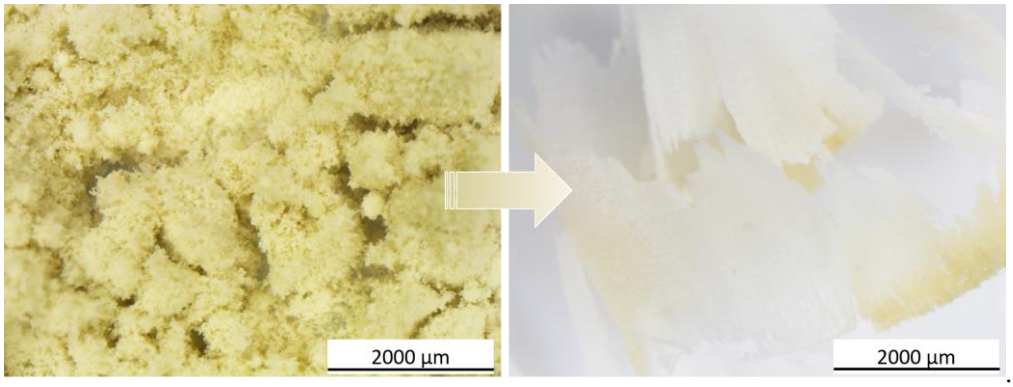

Figure 6. Bio-based additive aspect before and after the UV-B chamber exposure test.

Therefore, given the observed significant degradation of the bio-based additive, it becomes evident why the coatings G5, G10, and G10U exhibit distinct color changes as depicted in Figure 5b. Specifically, Figure 7 illustrates the progression of individual color coordinates of the samples during the accelerated degradation test. The loss of the green tea color within the composite additive leads to an increase in the brightness of the composite coatings, as demonstrated by the L* graph (Figure 7a). Simultaneously, the initial green hue (indicated by negative values of a* in Figure 7b) tends to cancel out, along with a reduction in the yellow component (Figure 7c). The inverse trends observed in the three coordinates of sample G0 compared to those of the three composite samples further underscore that the color loss in the coatings is primarily attributed to the degradation of the green component of the bio-based additive.

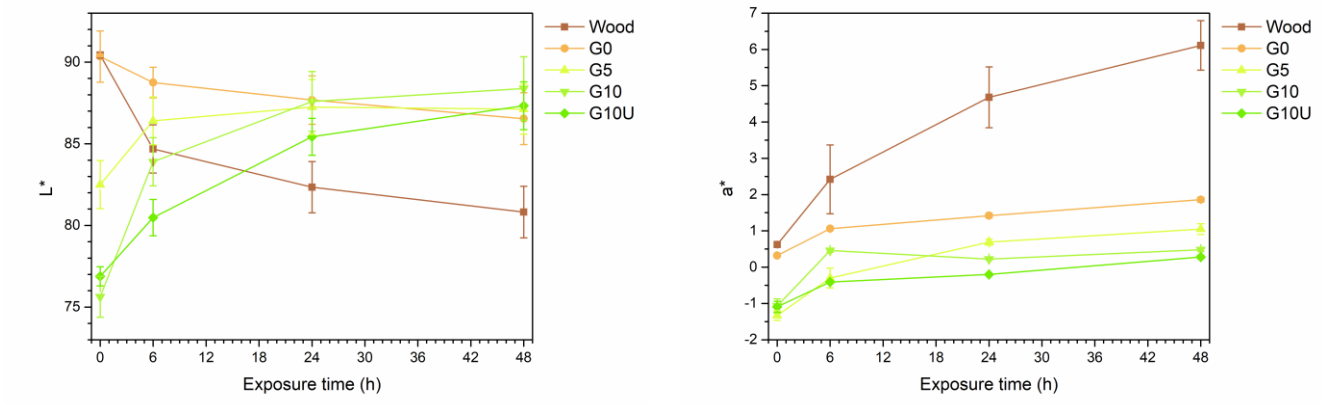

(**a**) (**b**)

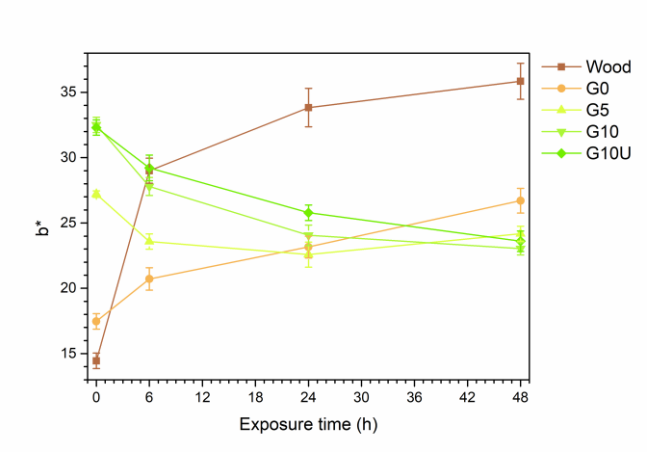

(**c**)

Figure 7. Evolution of the values of the specific CIE Lab coordinates (**a**) L*, (**b**) a*, and (**c**) b* during the UV-B chamber exposure test.

Hence, the coloring element of the bio-based additive, such as the infusion of green tea, emerges as a crucial factor that may constrain its use in paints intended for outdoor use, exposed directly to solar radiation.

Nevertheless, temperature also holds significant degrading potential. Therefore, the samples underwent specific thermal cycles in a climatic chamber to further explore this aspect. As per UNI 9429 standard practice, whitening phenomena and crack development are pivotal factors in assessing the durability of coatings exposed to environments with pronounced thermal fluctuations [59]. Hence, the samples underwent colorimetric measurements during the test, and at the conclusion of the experiment, their surfaces were scrutinized under an optical microscope to assess the presence of possible defects. Figure 8a illustrates the progression of color change in the different samples during the test. With the exception of the wooden panel, the four coated samples exhibit ΔE values that plateau below unity, and are hence considered almost negligible and not visually perceptible. These values are slightly higher in the presence of the bio-based additive, suggesting that its colored component may experience minor effects from temperature changes [67], albeit in residual quantities. Indeed, the examination of the trends in the values of a* in Figure 8b and b* in Figure 8c does not reveal any pronounced whitening phenomena in the coatings. Only a* is directed towards neutral values (0), but it does not indicate the complete loss of the coloring components of the pigment.

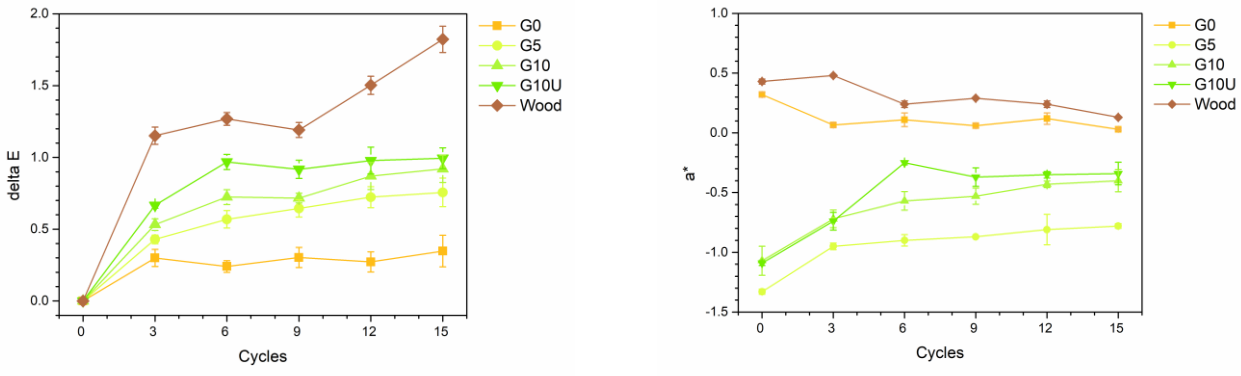

(**a**) (**b**)

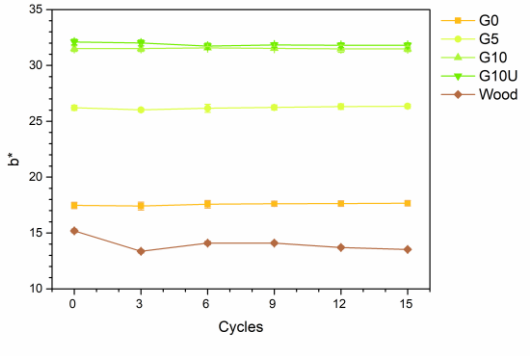

(**c**)

Figure 8. Change in (**a**) color, (**b**) coordinate a*, and (**c**) coordinate b* of the samples during the climatic chamber test.

Similarly, the surfaces of the samples do not exhibit specific defects induced by thermal changes, such as cracks, as demonstrated by the images in Figure 9. These images were captured using an optical microscope equipped with a polarizing filter at 4× magnification, as recommended by the standard, and at higher magnifications, such as 15× (shown on the right side of the images). No critical issues were observed at any magnification. Indeed, the images underscore the morphological contribution of the wax-based additive in mitigating surface reflectance phenomena of the coating, as previously elucidated and demonstrated by the analyses in Figure 3a.

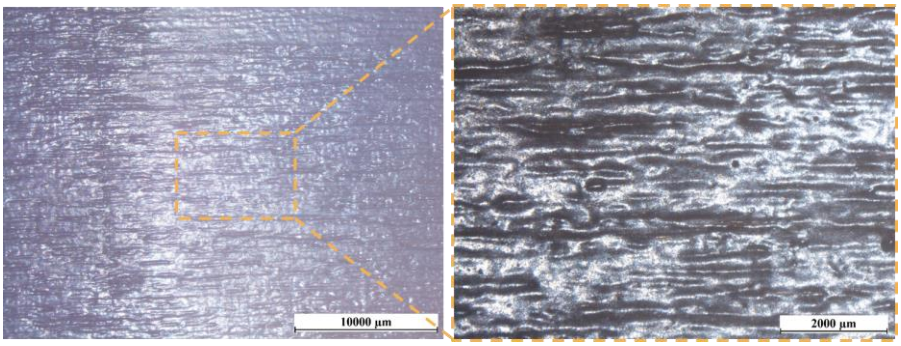

(**a**)

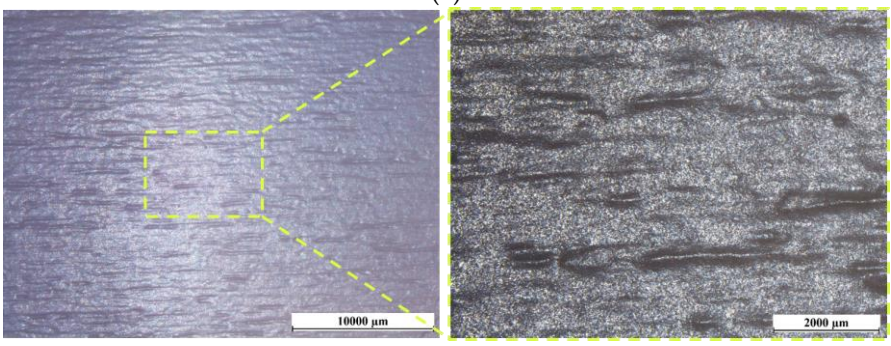

(**b**)

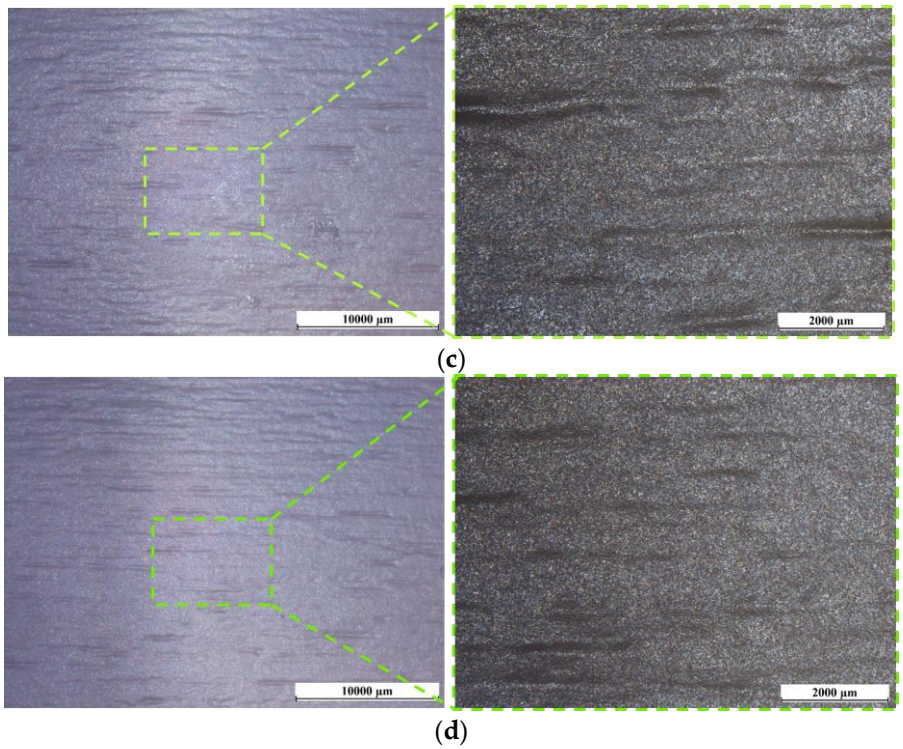

Figure 9. Optical micrographs of (**a**) sample G0, (**b**) sample G5, (**c**) sample G10, and (**d**) sample G10U acquired after the climatic chamber test at 4× (on the left) and 15× (on the right) magnification.

Hence, taking into account the parameters and categories delineating the extent of whitening and defects outlined in Table 2, as per the reference standard [59], all series of samples manifest category 0 for both phenomena. This signifies the absence of whitening and cracks across the samples. This finding emphasizes that the samples remain largely unaffected by thermal changes, as they do not experience notable decay. Moreover, the thermal variations do not induce aesthetic degradation of the bio-based additive. Additionally, the wax-based powder infused with green tea does not promote crack formation, demonstrating its good compatibility with the acrylic coating matrix.

Table 2. Classification of whitening phenomena and crack development observed during the climatic chamber exposure test.

Category	Whitening Phenomena	Crack Development
0	No whitening	No alterations
1	Light whitening	Defects perceptible solely with a 4× optical system
2	Intense whitening	Visible fissures

Ultimately, direct exposure to UV-B radiation poses considerable challenges for the bio-based additive, resulting in significant degradation of its colored component. Consequently, this results in avoidable aesthetic alterations to the coatings, warranting caution against outdoor application, even with the presence of the UV absorber, whose protective effect is limited. However, temperature fluctuations do not pose significant issues for the coatings, as they retain their aesthetic characteristics and physical integrity.

3.3. Effect of the Filler on the Barrier Properties of the Coatings

The inherent water-resistant properties of wax-based additives [78], along with their hydrophobic characteristics [79], are acknowledged for their effectiveness in reducing the absorption of aqueous solutions within wood coatings [32,34,80,81]. Hence, the samples

underwent water uptake tests to validate the protective efficacy of the wax-based additive. Figure 10 illustrates the progression of water absorption by the samples during the test, with the poplar wood panel serving as a reference to underscore the barrier function of the various coatings. Indeed, the amount of solution absorbed by the wood panel is significantly higher than that observed in the four series of coated samples. The coated samples exhibit a gradual absorption, which decreases slowly over time, indicating a potential saturation of the protective layers. Simultaneously, there is a noticeable distinction in behavior between sample G0 and the three samples containing the wax-based additive. The latter exhibits superior barrier characteristics, evidenced by a reduced amount of water uptake. Additionally, samples G5 and G10 demonstrate comparable outcomes, indicating that 5 wt.% of wax-based additive is adequate to significantly enhance the barrier properties of the acrylic coating. Indeed, at the conclusion of the test, sample G5 demonstrated a decrease in water uptake of approximately 25% compared to sample G0. The error bars show remarkably tight values, indicating a high degree of consistency in the results. Similar findings were previously emphasized in a prior study [34], reaffirming the excellent barrier properties of rice bran wax.

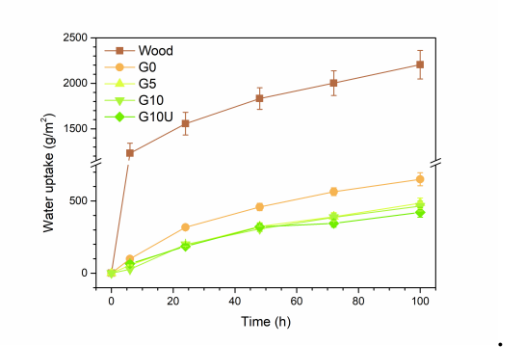

Figure 10. Water uptake evolution during the test.

Indeed, the decreased water absorption not only enhances the barrier properties but also contributes to the improved aesthetic integrity of the coating. As depicted in the graphs in Figure 11, the three series of composite coatings exhibit minimal color change (Figure 11a) and reflectance characteristics (Figure 11b), which remain largely unaffected by the water uptake test. The heightened absorption of solution in the pure acrylic matrix coating (sample G0) correlates with a noticeable color change and a decrease in the surface's reflectance properties. The substantial presence of the bio-based additive powder within the bulk of the coating of sample G10, as observed in Figure 4c, initially raised concerns about the potential percolation phenomena of aggressive solutions at the interface with the coating matrix. However, these results demonstrate the excellent compatibility of the additive with the acrylic resin, as previously confirmed by the exposure test in a climatic chamber.

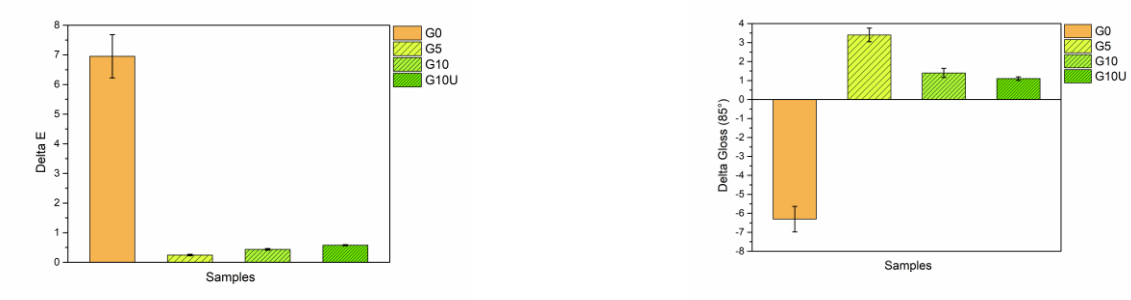

(**a**) (**b**)

Figure 11. Change in (**a**) color and (**b**) gloss due to the water uptake test.

Nevertheless, to better assess the superficial effects of contact with aggressive solutions, the samples underwent resistance tests to cold liquids. The results are depicted in Figure 12, showcasing the change in color (Figure 12a) and gloss (Figure 12b). The standard deviation values indicate good reproducibility of the measurements and stable behavior of the samples. According to the reference table of the standard [82], all samples exhibit excellent results, with color fading levels classified as 0-1, indicating either absent or minimal discoloration. Aside from contact with coffee, the coatings containing the green additive consistently display a slight rise in color change compared to sample G0. This is probably because tea extract is prone to discoloration when exposed for an extended period (96 h) to both aqueous and non-aqueous solutions, particularly under extreme pH conditions [77], such as those tested in this experiment (pH 1 and pH 14). Despite the tea-based additive component's susceptibility, the samples exhibited favorable behavior, including in terms of gloss (Figure 12b). With the exception of olive oil, which tends to enhance the reflectance of the composite coatings, counteracting the mattifying effect of the wax, the three series of samples G5, G10, and G10U demonstrated minimal variations in gloss, certainly lower than those observed in sample G0.

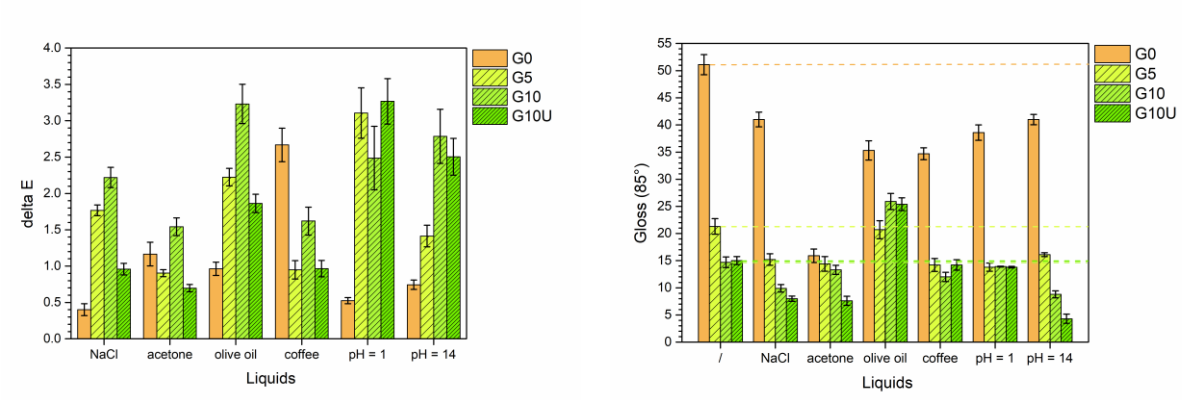

(**a**) (**b**)

Figure 12. Change in (**a**) coloration and (**b**) development of gloss of the samples after the liquid resistance test.

Finally, to evaluate the hydrophobic contribution of the wax-based additive, the samples were subjected to contact angle measurements. Table 3 presents the findings, emphasizing a distinct effect brought about by the bio-based additive. Specifically, the inclusion of the wax-based powder leads to a gradual increase in contact angle values. The addition of 5 wt.% and 10 wt.% of the additive results in approximately 8° and 12° increases in angle, respectively, thereby enhancing the hydrophobic characteristics of the rice bran wax. Previous studies in the literature have linked hydrophobic–hydrophilic traits to surface roughness levels [83,84]. Nonetheless, examination of Figure 3b reveals consistent surface morphology across all four sample series. Thus, the significant contact angle disparities observed in samples G5 and G10 are solely attributed to the hydrophobic nature of the wax, a trait extensively established in prior research [34,79]. Moreover, the outcome exhibited by sample G10U warrants particular attention as it aligns closely with that of sample G10. This similarity underscores the significant role played by the UV absorber, demonstrating its capacity to positively impact the coating without adversely affecting other properties. Indeed, it confirms that the UV absorber does not compromise the functional characteristics of the wax-based additive, ensuring the preservation of its functional features. Nevertheless, given the relatively low contact angle values observed across all four series of samples, it becomes challenging to definitively attribute hydrophobic properties to their surfaces [85]. Nonetheless, it is crucial not to underestimate the significant impact of the green additive, which demonstrates the capability to notably elevate the contact angle.

Table 3. Results of the contact angle measurements (θ).

Sample	Θ (°)
G0	51.6 ± 2.2
G5	59.9 ± 2.9
G10	63.4 ± 3.2
G10U	61.8 ± 3.5

In summary, the tests conducted underscored the effective barrier function of the coatings, which is bolstered by the inclusion of the green wax-based additive. This additive plays a crucial role in minimizing water absorption, thus maintaining the chromatic and aesthetic integrity of the composite layer even after prolonged exposure to harsh substances. While the surfaces may not exhibit purely hydrophobic properties, the protective efficacy of the bio-based additive remains clear, and its performance is unaffected by the simultaneous presence of the UV absorber.

3.4. Effect of the Filler on the Abrasion Resistance Properties of the Coatings

The effect of the wax-based additive on abrasion resistance properties was assessed using a scrub test, with results depicted in Figure 13. The graph shows the evolution of the loss in coating mass per unit area, defined as L, and calculated according to the formula:

$$L = (m_0 - m_n)/A \quad (2)$$

where m_0 and m_n represent the weight of the sample before the test and after the nth cycle of scrubbing, respectively, while A denotes the surface area affected by the abrasion caused by the movement of the abrasive sponge.

Since the test simulates mild scrubbing processes like repetitive surface cleaning rather than aggressive abrasion, initial distinctions among sample results become discernible only after the first 250 cycles, gradually magnifying as the test progresses. Indeed, it is evident that the mass lost during the test by sample G0 consistently exceeds that of the three composite coatings. This outcome underscores the effective protective function provided by the wax-based filler. By the conclusion of the test, the enhancement achieved by the 5 wt.% and 10 wt.% of wax, in terms of reducing mass loss compared to the reference sample G0, equated to about 13% and 19%, respectively. Similar findings have been previously documented in studies examining the protective function of wax-based fillers in wood paints [32,34]. However, other literature on the utilization of bio-based additives has not consistently exhibited such reinforcing effects. For instance, polyamide 11 powders show less conspicuous contributions [68], while cellulose fibers may even diminish protective performances due to agglomeration issues of the additive [35]. Consequently, wax-based powders emerge as promising reinforcing fillers [86], often showcasing superior protective performances compared to other bio-based additives for wood paints available in the market [3]. In conclusion, the UV absorber does not demonstrate any notable impact on abrasion resistance. The performance of sample G10U remains comparable to that of samples G5 and G10, indicating that the presence of the UV absorber does not significantly alter the abrasion resistance properties observed in the coatings.

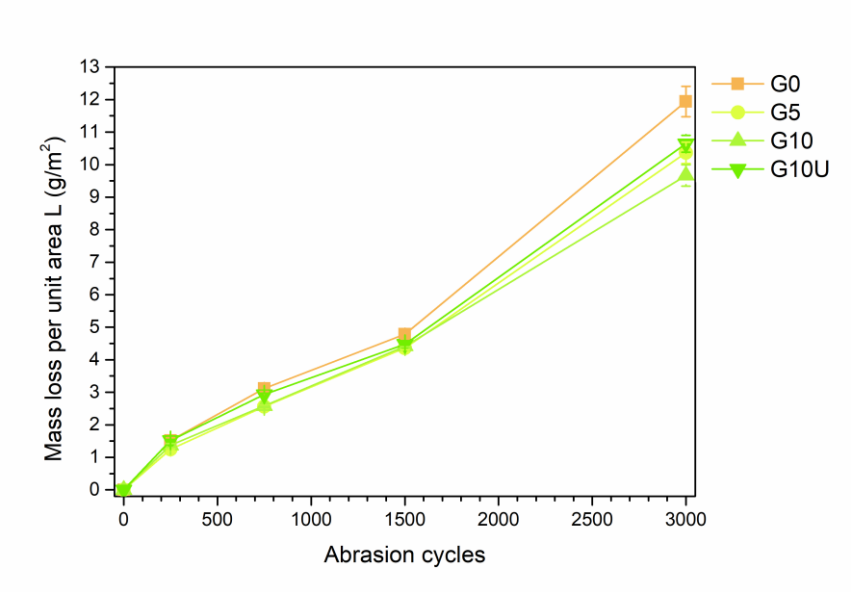

Figure 13. Evolution of the mass loss per unit area L during the scrub test.

Certainly, the abrasive processes can impact the aesthetic qualities of the coatings. Therefore, the color and gloss consistency of the samples were monitored throughout the scrub test. Figure 14a illustrates the progression of color change in the samples. Given the notably low values observed, it can be concluded that the abrasive phenomenon does not significantly influence the color of the bio-based additive, which retains its green–yellow hue consistently throughout the test. The abrasive process does indeed influence the reflectance properties, as evidenced by the graph depicting the evolution of gloss in Figure 14b. The acrylic matrix experiences a reduction in reflectance (as observed in sample G0), whereas the composite coatings demonstrate a slight increase in gloss throughout the abrasive test. This phenomenon is less pronounced in samples G10 and G10U, where the high concentration of wax-based filler maintains strong opacity, thereby mitigating the effects on gloss. These phenomena can be elucidated by the morphological changes induced by the abrasion process of the scrub sponge, as indicated by the surface roughness measurements depicted in Figure 14c. The graph illustrates the progression of roughness values both parallel (Ra//) and perpendicular (Ra⊥) to the fibers of the wooden substrate. The roughness values parallel to the substrate fibers (Ra//) remain consistent throughout the test, as the abrasive sponge moves in the same direction as the fibers. Consequently, its movement does not induce significant morphological defects in this direction. Conversely, the values of Ra⊥ are partially altered due to the rubbing action of the abrasive sponge. This phenomenon is notably evident in sample G0, where the values of Ra⊥ undergo a substantial increase during the test, indicating significant morphological alterations. In contrast, this effect is less pronounced in coatings containing the bio-based filler, and in some instances, there is even a reduction in roughness, suggesting a smoothing or "flattening" of the surface. Hence, apart from the increased material loss, the abrasive process also induces significant changes in the surface morphology of the acrylic matrix. Both of these phenomena appear to be effectively mitigated by the wax-based additive.

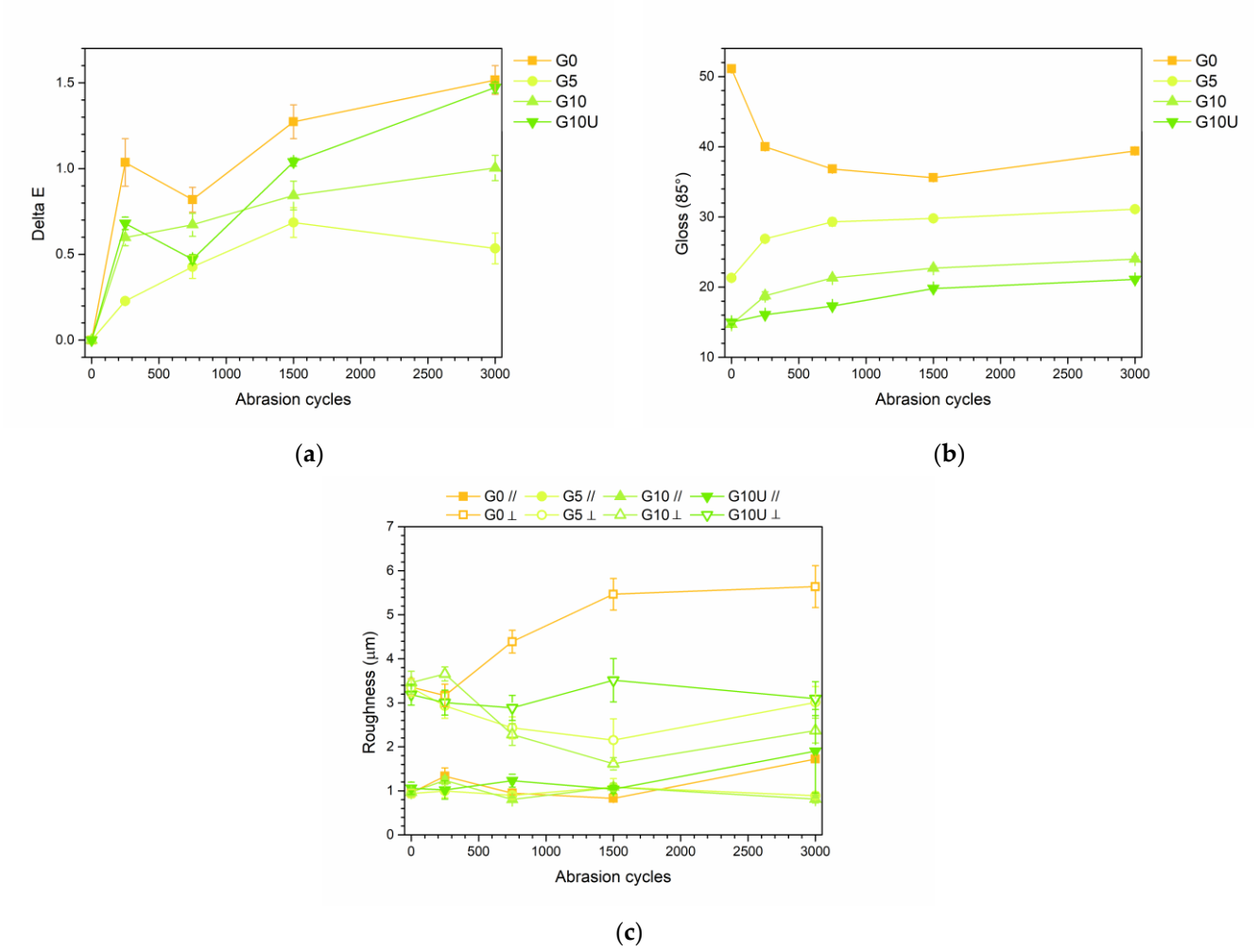

Figure 14. Evolution of (**a**) color, (**b**) gloss, and (**c**) roughness (longitudinal//and perpendicular ⊥) during the scrub test.

To further scrutinize the protective contribution of the filler, the samples were subsequently examined under scanning electron microscopy (SEM) at the conclusion of the test. Figure 15 displays the surface appearance of the coatings after undergoing 3000 scrub test cycles. The images vividly depict a distinct morphological contrast between sample G0 and the three composite coatings. Sample G0 appears significantly impacted by the abrasion process, displaying evident surface deformations characterized by typical abrasion lines caused by the scrub sponge [87,88]. These observations help elucidate the observed increase in Ra⊥ values illustrated in the graph of Figure 14c. In contrast, the gradual inclusion of wax-based powder results in a specific phenomenon, as noted in prior research [32,34]: the motion of the scrubbing pad does not remove material; rather, it triggers the plastic deformation of the rice bran wax, known for its pliability even at room temperature [89]. This behavior is characteristic of wax-based additives commonly used to create smooth surfaces [90]. The pad tends to disperse the wax, occasionally reducing the values of Ra⊥, thereby mitigating friction between the coating surface and the pad itself. As a result, the wax's reinforcing capability arises from its capacity to undergo plastic deformation, thereby reducing surface friction. Thus, the coating experiences diminished material loss, as evidenced in Figure 13, as it is not entirely stripped away by the pad but rather spread across the surface of the composite layer. Polyamide 11-based additives exhibit a comparable phenomenon [68], indicating that materials capable of plastic deformation during third-body streaking processes can notably enhance the abrasion resistance of wood coatings.

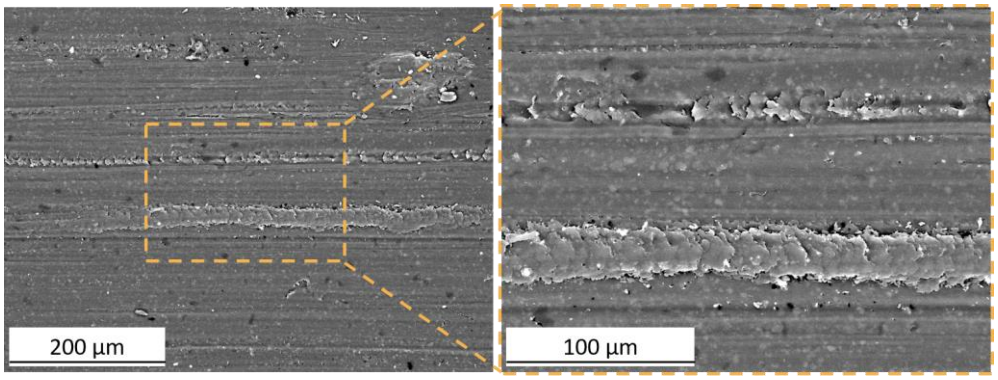

(**a**)

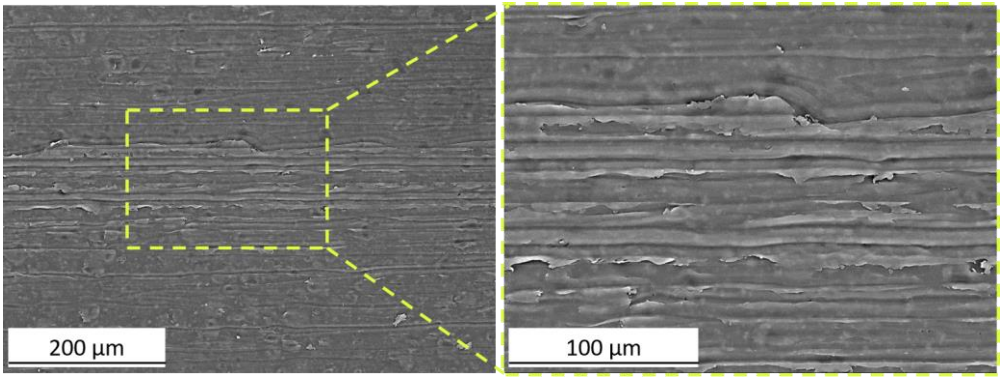

(**b**)

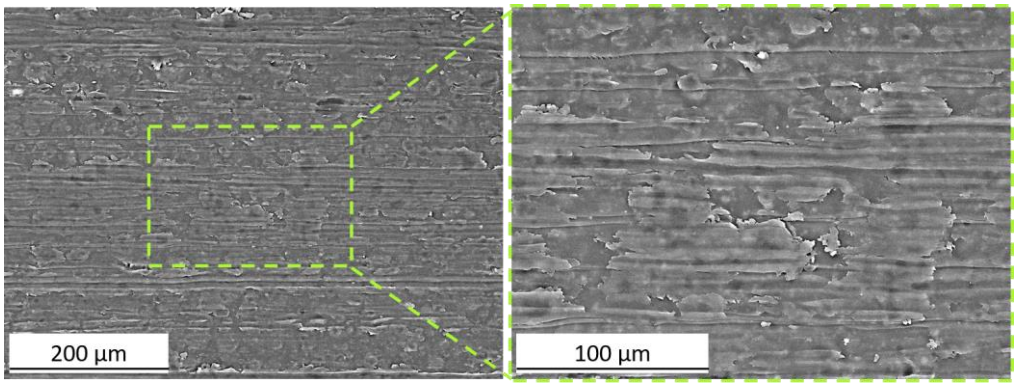

(**c**)

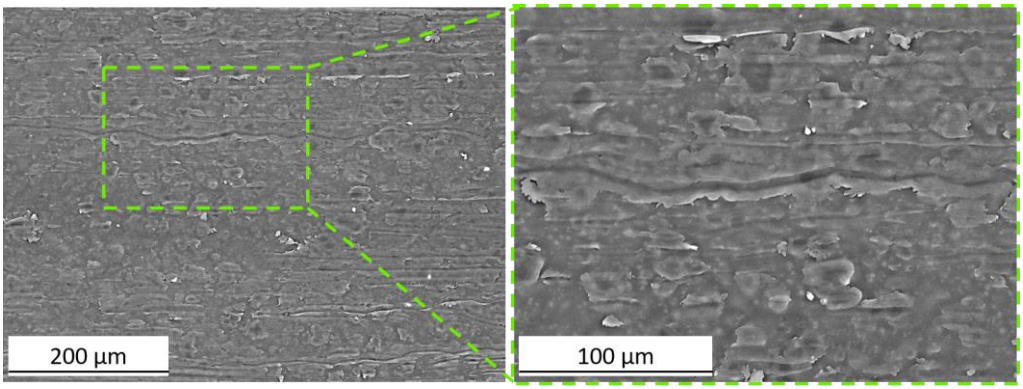

(**d**)

Figure 15. SEM micrographs of the surface morphology of (**a**) sample G0, (**b**) sample G5, (**c**) sample G10, and (**d**) sample G10U, acquired after 3000 cycles of scrub test.

In summary, the bio-based additive reaffirms the established reinforcing capabilities of wax-based fillers, effectively reducing mass loss in coatings subjected to abrasion. The shear stresses generated by the abrasive sponge's movement result in the plastic deformation of the powder, preserving the surface morphology of the coating. Consequently, the green additive demonstrates additional protective functionality, complementing its specific color and barrier effect, making it particularly appealing for use in wood paints.

4. Conclusions

This study examined the suitability of a bio-derived additive composed of rice bran wax infused with green tea as an environmentally sustainable and versatile pigment for wood paints. Additionally, the bio-based additive was evaluated in combination with a dedicated UV absorber, included to enhance the color consistency of the wax-based powder when exposed to solar radiation. The additive exhibited effective coloring capabilities attributed to the green–yellow tones from the green tea infusion, along with mattifying properties contributed by the wax component.

However, direct exposure to UV-B radiation led to considerable loss of the colored component, compromising the aesthetic appeal of the coatings. As a result, caution is advised against outdoor application, despite the presence of the UV absorber, which provided some protective benefits but had limitations. On the other hand, fluctuations in temperature did not significantly impact the coatings, as they maintained their aesthetic qualities and structural integrity.

Different tests focused on assessing the barrier properties of the bio-based additive have consistently highlighted the protective function of the coatings, which is further enhanced by incorporating green wax-based powder. This additive plays a pivotal role in reducing water absorption, thereby preserving the color and aesthetic appeal of the composite layer even after prolonged exposure to harsh conditions. Although the surfaces may not display purely hydrophobic characteristics, the protective effectiveness of the bio-based additive remains evident, and its performance remains unaffected by the concurrent presence of the UV absorber.

Ultimately, the bio-based additive confirms the established reinforcing qualities of wax-based fillers, effectively reducing material loss in coatings subjected to rigorous abrasion. The movement of the abrasive sponge causes shear stresses that result in the plastic deformation of the powder, maintaining the surface morphological structure of the coating.

In conclusion, the *green* additive showcases its versatility as a multifunctional pigment, providing not just color improvement but also robust protective features. Its distinctive mix of color, mattifying impact, barrier enhancement, and protective function makes it highly appealing for application as a functional bio-based additive in wood paints. Therefore, this study paves the way for further research into the impact of other types of wax-based fillers in paints, leveraging the intriguing functionalities highlighted by rice bran wax. The infusion with green tea offers the ability to adjust the final color of the coating based on the amount of filler added. However, the findings indicate that 5 wt.% of additive suffices to achieve desired coloring and effective protective properties. Future studies will undoubtedly be required to develop effective solutions for limiting the degradation of the bio-based pigment when exposed outdoors. Nonetheless, the application of UV absorbers in this study has yielded promising insights.

Author Contributions: Conceptualization, M.C. and S.R.; methodology, M.C. and S.R.; investigation, M.C.; data curation, M.C. and S.R.; writing—original draft preparation, M.C.; writing—review and editing, M.C. and S.R.; supervision, S.R. All authors have read and agreed to the published version of the manuscript.

Funding: This research received no external funding.

Institutional Review Board Statement: Not applicable.

Informed Consent Statement: Not applicable.

Data Availability Statement: The data presented in this study are available on request from the corresponding author. The data are not publicly available due to the absence of an institutional repository.

Acknowledgments: The authors greatly acknowledge the contributions of Stefano Di Blase (ICA Group, Civitanova Marche, MC, Italy) for the paint supply. Moreover, special thanks should be given to Gianluca Cometti (Azelis Italia, Milan, Italy) and Donna Gilbert (Micro Powders, Tarrytown, NY, USA) for the supply of the composite wax-based additive. The publication was created with the co-financing of the European Union, FSE-REACT-EU, and PON Research and Innovation 2014–2020 DM1062/2021.

Conflicts of Interest: The authors declare no conflicts of interest.

Appendix A

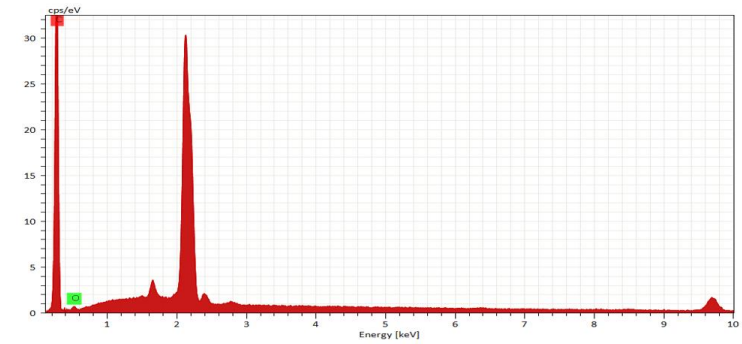

Name	Date	Time	HV [kV]	Real time [s]	Dead time [%]	Pulses [kcps]
Cera-the.spx	1/31/2024	3:16:49 PM	15.0	40.000	9	15.686

Element	At. No.	Netto	Mass [%]	Mass Norm. [%]	Atom [%]	abs. error [%] (1 sigma)	rel. error [%] (1 sigma)
Carbon	6	77430	96.37	96.37	97.25	11.02	11.44
Oxygen	8	724	3.63	3.63	2.75	0.90	24.86
		Sum	**100.00**	**100.00**	**100.00**		

Figure A1. EDXS analysis of the bio-based additive.

References

1. Sadh, P.K.; Duhan, S.; Duhan, J.S. Agro-industrial wastes and their utilization using solid state fermentation: A review. *Bioresour. Bioprocess* **2018**, *5*, 1.
2. Sanjay, M.; Madhu, P.; Jawaid, M.; Senthamaraikannan, P.; Senthil, S.; Pradeep, S. Characterization and properties of natural fiber polymer composites: A comprehensive review. *J. Clean. Prod.* **2018**, *172*, 566–581.
3. Calovi, M.; Zanardi, A.; Rossi, S. Recent Advances in Bio-Based Wood Protective Systems: A Comprehensive Review. *Appl. Sci.* **2024**, *14*, 736.
4. Patil, A.M.; Jagtap, R.N. PU-coating performance of bio-based hyperbranched alkyd resin on mild steel and wood substrate. *J. Coat. Technol. Res.* **2021**, *18*, 741–752.
5. Kartal, S.N.; Hwang, W.-J.; Imamura, Y.; Sekine, Y. Effect of essential oil compounds and plant extracts on decay and termite resistance of wood. *Eur. J. Wood Wood Prod.* **2006**, *64*, 455–461.
6. Humar, M.; Lesar, B. Efficacy of linseed-and tung-oil-treated wood against wood-decay fungi and water uptake. *Int. Biodeterior. Biodegrad.* **2013**, *85*, 223–227.
7. Arminger, B.; Jaxel, J.; Bacher, M.; Gindl-Altmutter, W.; Hansmann, C. On the drying behavior of natural oils used for solid wood finishing. *Prog. Org. Coat.* **2020**, *148*, 105831.
8. Shang, Q.; Chen, J.; Liu, C.; Hu, Y.; Hu, L.; Yang, X.; Zhou, Y. Facile fabrication of environmentally friendly bio-based superhydrophobic surfaces via UV-polymerization for self-cleaning and high efficient oil/water separation. *Prog. Org. Coat.* **2019**, *137*, 105346.
9. Rosu, D.; Bodîrlău, R.; Teacă, C.A.; Rosu, L.; Varganici, C.D. Epoxy and succinic anhydride functionalized soybean oil for wood protection against UV light action. *J. Clean. Prod.* **2016**, *112*, 1175–1183.
10. Walsh-Korb, Z.; Stelzner, I.; dos Santos Gabriel, J.; Eggert, G.; Avérous, L. Morphological Study of Bio-Based Polymers in the Consolidation of Waterlogged Wooden Objects. *Materials* **2022**, *15*, 681.
11. Lu, J.; Venäläinen, M.; Julkunen-Tiitto, R.; Harju, A.M. Stilbene impregnation retards brown-rot decay of Scots pine sapwood. *Holzforschung* **2016**, *70*, 261–266.
12. Barbero-López, A.; Chibily, S.; Tomppo, L.; Salami, A.; Ancin-Murguzur, F.J.; Venäläinen, M.; Lappalainen, R.; Haapala, A. Pyrolysis distillates from tree bark and fibre hemp inhibit the growth of wood-decaying fungi. *Ind. Crops Prod.* **2019**, *129*, 604–610.

13. Yildiz, Ü.C.; Kiliç, C.; Gürgen, A.; Yildiz, S. Possibility of using lichen and mistletoe extracts as potential natural wood preservative. *Maderas. Cienc. Tecnol.* **2020**, *22*, 179–188.
14. Šimůnková, K.; Reinprecht, L.; Nábělková, J.; Hýsek, Š.; Kindl, J.; Borůvka, V.; Lišková, T.; Šobotník, J.; Pánek, M. Caffeine–Perspective natural biocide for wood protection against decaying fungi and termites. *J. Clean. Prod.* **2021**, *304*, 127110.
15. De Medeiros, F.C.; Gouveia, F.N.; Bizzo, H.R.; Vieira, R.F.; Del Menezzi, C.H. Fungicidal activity of essential oils from Brazilian Cerrado species against wood decay fungi. *Int. Biodeterior. Biodegrad.* **2016**, *114*, 87–93.
16. Xie, Y.; Wang, Z.; Huang, Q.; Zhang, D. Antifungal activity of several essential oils and major components against wood-rot fungi. *Ind. Crops Prod.* **2017**, *108*, 278–285.
17. Anttila, A.-K.; Pirttilä, A.M.; Häggman, H.; Harju, A.; Venäläinen, M.; Haapala, A.; Holmbom, B.; Julkunen-Tiitto, R. Condensed conifer tannins as antifungal agents in liquid culture. *Holzforschung* **2013**, *67*, 825–832.
18. Silveira, A.G.; Santini, E.J.; Kulczynski, S.M.; Trevisan, R.; Wastowski, A.D.; Gatto, D.A. Tannic extract potential as natural wood preservative of *Acacia mearnsii*. *An. Acad. Bras. Cienc.* **2017**, *89*, 3031–3038.
19. Tomak, E.; Gonultas, O. The wood preservative potentials of valonia, chestnut, tara and sulphited oak tannins. *J. Wood Chem. Technol.* **2018**, *38*, 183–197.
20. Marrot, L.; Zouari, M.; Schwarzkopf, M.; DeVallance, D.B. Sustainable biocarbon/tung oil coatings with hydrophobic and UV-shielding properties for outdoor wood substrates. *Prog. Org. Coat.* **2023**, *177*, 107428.
21. Zikeli, F.; Vinciguerra, V.; D'Annibale, A.; Capitani, D.; Romagnoli, M.; Scarascia Mugnozza, G. Preparation of lignin nanoparticles from wood waste for wood surface treatment. *Nanomaterials* **2019**, *9*, 281.
22. Tomak, E.D.; Arican, F.; Gonultas, O.; Parmak, E.D.S. Influence of tannin containing coatings on weathering resistance of wood: Water based transparent and opaque coatings. *Polym. Degrad. Stab.* **2018**, *151*, 152–159.
23. Jusic, J.; Tamantini, S.; Romagnoli, M.; Vinciguerra, V.; Di Mattia, E.; Zikeli, F.; Cavalera, M.; Scarascia Mugnozza, G. Improving sustainability in wood coating: Testing lignin and cellulose nanocrystals as additives to commercial acrylic wood coatings for bio-building. *iForest* **2021**, *14*, 499.
24. Tamantini, S.; Bergamasco, S.; Zikeli, F.; Humar, M.; Cavalera, M.; Romagnoli, M. Cellulose Nano Crystals (CNC) as Additive for a Bio-Based Waterborne Acrylic Wood Coating: Decay, Artificial Weathering, Physical and Chemical Tests. *Nanomaterials* **2023**, *13*, 442.
25. Kaboorani, A.; Auclair, N.; Riedl, B.; Landry, V. Physical and morphological properties of UV-cured cellulose nanocrystal (CNC) based nanocomposite coatings for wood furniture. *Prog. Org. Coat.* **2016**, *93*, 17–22.
26. Barbero-López, A.; Ochoa-Retamero, A.; López-Gómez, Y.; Vilppo, T.; Venäläinen, M.; Lavola, A.; Julkunen-Tiitto, R.; Haapala, A. Activity of spent coffee ground cinnamates against wood-decaying fungi in vitro. *BioResources* **2018**, *13*, 6555–6564.
27. Woźniak, M.; Kwaśniewska-Sip, P.; Waśkiewicz, A.; Cofta, G.; Ratajczak, I. The possibility of propolis extract application in wood protection. *Forests* **2020**, *11*, 465.
28. Moutaouafiq, S.; Farah, A.; Ez zoubi, Y.; Ghanmi, M.; Satrani, B.; Bousta, D. Antifungal activity of *Pelargonium graveolens* essential oil and its fractions against wood decay fungi. *J. Essent. Oil-Bear. Plants* **2019**, *22*, 1104–1114.
29. Wiemann, M.C. Characteristics and availability of commercially important woods. In *Wood Handbook: Wood as an Engineering Material*; Forest Products Laboratory: Madison, WI, USA; United States Department of Agriculture Forest Service: Madison, WI, USA, 2010.
30. Yan, X.; Chang, Y.; Qian, X. Effect of the concentration of pigment slurry on the film performances of waterborne wood coatings. *Coatings* **2019**, *9*, 635.
31. Yan, X.; Wang, L.; Qian, X. Influence of thermochromic pigment powder on properties of waterborne primer film for Chinese fir. *Coatings* **2019**, *9*, 742.
32. Calovi, M.; Rossi, S. Synergistic contribution of bio-based additives in wood paint: The combined effect of pigment deriving from spirulina and multifunctional filler based on carnauba wax. *Prog. Org. Coat.* **2023**, *182*, 107713.
33. Calovi, M.; Rossi, S. Comparative analysis of the advantages and disadvantages of utilizing spirulina-derived pigment as a bio-based colorant for wood impregnator. *Coatings* **2023**, *13*, 1154.
34. Calovi, M.; Rossi, S. Eco-Friendly Multilayer Coating Harnessing the Functional Features of Curcuma-Based Pigment and Rice Bran Wax as a Hydrophobic Filler. *Materials* **2023**, *16*, 7086.
35. Calovi, M.; Rossi, S. Impact of High Concentrations of Cellulose Fibers on the Morphology, Durability and Protective Properties of Wood Paint. *Coatings* **2023**, *13*, 721.
36. Liu, Y.; Yu, Z.; Zhang, Y.; Qi, C.; Tang, R.; Zhao, B.; Wang, H.; Han, Y. Microbial dyeing—Infection behavior and influence of *Lasiodiplodia theobromae* in poplar veneer. *Dye. Pigment.* **2020**, *173*, 107988.
37. Liu, Y.; Zhang, Y.; Yu, Z.; Qi, C.; Tang, R.; Zhao, B.; Wang, H.; Han, Y. Microbial dyes: Dyeing of poplar veneer with melanin secreted by *Lasiodiplodia theobromae* isolated from wood. *Appl. Microbiol. Biotechnol.* **2020**, *104*, 3367–3377.
38. Nikitha, M.; Natarajan, V. Properties of South-Indian rice cultivars: Physicochemical, functional, thermal and cooking characterisation. *J. Food Sci. Technol.* **2020**, *57*, 4065–4075.
39. Vali, S.R.; Ju, Y.-H.; Kaimal, T.N.B.; Chern, Y.-T. A process for the preparation of food-grade rice bran wax and the determination of its composition. *J. Am. Oil. Chem. Soc.* **2005**, *82*, 57–64.
40. Ghosh, M.; Bandyopadhyay, S. Studies on the crystal growth of rice bran wax in a hexane medium. *J. Am. Oil. Chem. Soc.* **2005**, *82*, 229–231.
41. Martini, S.; Añon, M.C. Crystallization of sunflower oil waxes. *J. Am. Oil. Chem. Soc.* **2003**, *80*, 525–532.
42. Ning, L.; Zhang, L.; Zhang, S.; Wang, W. How does surfactant affect the hydrophobicity of wax-coated wood? *Colloids Surf. A Physicochem. Eng. Asp.* **2022**, *650*, 129606.

43. Torun, I.; Ruzi, M.; Er, F.; Onses, M.S. Superhydrophobic coatings made from biocompatible polydimethylsiloxane and natural wax. *Prog. Org. Coat* **2019**, *136*, 105279.
44. Saji, V.S. Wax-based artificial superhydrophobic surfaces and coatings. *Colloids Surf. A Physicochem. Eng. Asp.* **2020**, *602*, 125132.
45. Namita, P.; Mukesh, R.; Vijay, K.J. *Camellia sinensis* (green tea): A review. *Glob. J. Pharmacol.* **2012**, *6*, 52–59.
46. Choi, M.-H.; Min, M.-J.; Oh, D.-S.; Shin, H.-J. Antimicrobial and antioxidant activity of *Camellia japonica* extracts for cosmetic applications. *KSBB J.* **2013**, *28*, 99–105.
47. Becker, L.C.; Bergfeld, W.F.; Belsito, D.V.; Hill, R.A.; Klaassen, C.D.; Liebler, D.C.; Marks, J.G., Jr.; Shank, R.C.; Slaga, T.J.; Snyder, P.W. Safety Assessment of *Camellia sinensis*–Derived Ingredients as Used in Cosmetics. *Int. J. Toxicol.* **2019**, *38*, 48S–70S.
48. Koch, W.; Zagórska, J.; Marzec, Z.; Kukula-Koch, W. Applications of tea (*Camellia sinensis*) and its active constituents in cosmetics. *Molecules* **2019**, *24*, 4277.
49. Šimon, P.; Fratričová, M.; Schwarzer, P.; Wilde, H.-W. Evaluation of the residual stability of polyurethane automotive coatings by DSC: Equivalence of Xenotest and desert weathering tests and the synergism of stabilizers. *J. Therm. Anal. Calorim.* **2006**, *84*, 679–692.
50. Queant, C.; Landry, V.; Blanchet, P.; Schorr, D. Synthesis and incorporation of poly (methyl methacrylate) microspheres with UV stabilizers in wood clear coating binder. *J. Coat. Technol. Res.* **2017**, *14*, 1411–1422.
51. Liu, Y.; Liu, Y.; Lin, J.; Tan, H.; Zhang, C. UV-protective treatment for Vectran® fibers with hybrid coatings of TiO_2/organic UV absorbers. *J. Adhes. Sci. Technol.* **2014**, *28*, 1773–1782.
52. Shenoy, M.; Marathe, Y. Studies on synergistic effect of UV absorbers and hindered amine light stabilisers. *Pigm. Resin Technol.* **2007**, *36*, 83–89.
53. Aloui, F.; Ahajji, A.; Irmouli, Y.; George, B.; Charrier, B.; Merlin, A. Inorganic UV absorbers for the photostabilisation of woodclearcoating systems: Comparison with organic UV absorbers. *Appl. Surf. Sci.* **2007**, *253*, 3737–3745.
54. Balatinecz, J.J.; Kretschmann, D.E.; Leclercq, A. Achievements in the utilization of poplar wood–guideposts for the future. *For. Chron.* **2001**, *77*, 265–269
55. Balatinecz, J.J.; Kretschmann, D.E. Properties and utilization of poplar wood. In *Poplar Culture in North America*; NRC Research Press: Ottawa, Canada, 2001; pp. 277–291. ISBN: 978-0-660-18145-5.
56. Nikafshar, S.; Zabihi, O.; Ahmadi, M.; Mirmohseni, A.; Taseidifar, M.; Naebe, M. The effects of UV light on the chemical and mechanical properties of a transparent epoxy-diamine system in the presence of an organic UV absorber. *Materials* **2017**, *10*, 180.
57. *ASTM D523-14*; Standard Test Method for Specular Gloss. ASTM International: West Conshohocken, PA, USA, 2014; pp. 1–12.
58. *ASTM D4587-11(2019)e1*; Standard Practice for Fluorescent UV-Condensation Exposures of Paint and Related Coatings. ASTM International: West Conshohocken, PA, USA, 2019; pp. 1–6.
59. *UNI 9429-22*; Finiture del Legno e dei Mobili—Determinazione Della Resistenza Delle Superfici Agli Sbalzi di Temperatura. UNI-Ente Nazionale Italiano di Unificazione: Rome, Italy, 2022; pp. 1–11.
60. *EN927-05*; Paints and Varnishes—Coating Materials and Coating Systems for Exterior Wood-Part 5: Assessment of the liquid water permeability. European Standard: Brussels, Belgium, 2005; pp. 1–18.
61. *UNI EN 12720-14*; Assessment of Surface Resistance to Cold Liquids. European Committee for Standardization: Brussels, Belgium, 2014; pp. 1–4.
62. *ASTM D7334–08*; Standard Practice for Surface Wettability of Coatings, Substrates and Pigments by Advancing Contact Angle Measurement. ASTM International: West Conshohocken, PA, USA, 2008; pp. 1–3.
63. *ISO 11998-06*; Paints and Varnishes: Determination of Wet-Scrub Resistance and Cleanability of Coatings. BSI British Standards: London, UK, 2006; pp. 1–11.
64. *ASTM-E308-18*; Standard Practice for Computing the Colors of Objectives by Using the CIE System. ASTM International: West Conshohocken, PA, USA, 2018; pp. 1–45.
65. Mokrzycki, W.; Tatol, M. Colour difference ΔE—A survey. *Mach. Graph. Vis.* **2011**, *20*, 383–411.
66. Dai, Q.; He, Y.; Ho, C.-T.; Wang, J.; Wang, S.; Yang, Y.; Gao, L.; Xia, T. Effect of interaction of epigallocatechin gallate and flavonols on color alteration of simulative green tea infusion after thermal treatment. *J. Food. Sci. Technol.* **2017**, *54*, 2919–2928.
67. Wang, J.-Q.; Fu, Y.-Q.; Granato, D.; Yu, P.; Yin, J.-F.; Zeng, L.; Xu, Y.-Q. Study on the color effects of (-)-epigallocatechin-3-gallate under different pH and temperatures in a model beverage system. *Food Control* **2022**, *139*, 109112.
68. Calovi, M.; Rossi, S. Exploring polyamide 11 as a novel renewable resource-based filler in wood paint: Investigating aesthetic aspects and durability impact of the composite coating. *Prog. Org. Coat.* **2024**, *188*, 108262.
69. Calovi, M.; Rossi, S. Evaluating the versatility of stainless steel flakes and magnetite powder as polyvalent additives for wood paints. *J. Mater. Res. Technol.* **2024**, *29*, 1010–1024.
70. Calovi, M.; Rossi, S. From wood waste to wood protection: New application of black bio renewable water-based dispersions as pigment for bio-based wood paint. *Prog. Org. Coat.* **2023**, *180*, 107577.
71. Teacă, C.-A.; Roşu, D.; Bodîrlău, R.; Roşu, L. Structural Changes in Wood under Artificial UV Light Irradiation Determined by FTIR Spectroscopy and Color Measurements—A Brief Review. *BioResources* **2013**, *8*, 1478–1507.
72. Brischke, C.; Bayerbach, R.; Otto Rapp, A. Decay-influencing factors: A basis for service life prediction of wood and wood-based products. *Wood Mater. Sci. Eng.* **2006**, *1*, 91–107.
73. Kropat, M.; Hubbe, M.A.; Laleicke, F. Natural, accelerated, and simulated weathering of wood: A review. *BioResources* **2020**, *15*, 9998.
74. Calovi, M.; Coroneo, V.; Palanti, S.; Rossi, S. Colloidal silver as innovative multifunctional pigment: The effect of Ag concentration on the durability and biocidal activity of wood paints. *Prog. Org. Coat.* **2023**, *175*, 107354.
75. Yang, C.S.; Lambert, J.D.; Sang, S. Antioxidative and anti-carcinogenic activities of tea polyphenols. *Arch. Toxicol.* **2009**, *83*, 11–21.

76. Khan, N.; Mukhtar, H. Tea polyphenols for health promotion. *Life Sci.* **2007**, *81*, 519–533.
77. Zeng, L.; Ma, M.; Li, C.; Luo, L. Stability of tea polyphenols solution with different pH at different temperatures. *Int. J. Food Prop.* **2017**, *20*, 1–18.
78. Garai, R.M.; Sánchez, I.C.; García, R.T.; Rodríguez Valverde, M.; Cabrerizo Vílchez, M.; Hidalgo-Álvarez, R. Study on the effect of raw material composition on water-repellent capacity of paraffin wax emulsions on wood. *J. Dispers. Sci. Technol.* **2005**, *26*, 9–18.
79. Gupta, S.; Ivvala, J.; Grewal, H. Development of natural wax based durable superhydrophobic coatings. *Ind. Crops Prod.* **2021**, *171*, 113871.
80. Lozhechnikova, A.; Bellanger, H.; Michen, B.; Burgert, I.; Österberg, M. Surfactant-free carnauba wax dispersion and its use for layer-by-layer assembled protective surface coatings on wood. *Appl. Surf. Sci.* **2017**, *396*, 1273–1281.
81. Bang, J.; Kim, J.; Kim, Y.; Oh, J.-K.; KWAK, H.W. Preparation and characterization of hydrophobic coatings from carnauba wax/lignin blends. *J. Korean Wood Sci. Technol.* **2022**, *50*, 149–158.
82. *GB/T11186.3-90*; Method of Measurement of Coating Color. Part III: Calculation of Chromatic Aberration. Standardization Administration of the People's Republic of China: Beijing, China, 1990; pp. 1–12.
83. Wang, X.; Qu, Z.; Lai, T.; Ren, G.; Wang, W. Enhancing water transport performance of gas diffusion layers through coupling manipulation of pore structure and hydrophobicity. *J. Power Sources* **2022**, *525*, 231121.
84. Wang, X.; Qu, Z.; Ren, G. Collective enhancement in hydrophobicity and electrical conductivity of gas diffusion layer and the electrochemical performance of PEMFCs. *J. Power Sources* **2023**, *575*, 233077.
85. Law, K.-Y. Definitions for hydrophilicity, hydrophobicity, and superhydrophobicity: Getting the basics right. *J. Phys. Chem. Lett.* **2014**, *5*, 686–688.
86. Teaca, C.A.; Roşu, D.; Mustaţă, F.; Rusu, T.; Roşu, L.; Roşca, I.; Varganici, C.-D. Natural bio-based products for wood coating and protection against degradation: A Review. *BioResources* **2019**, *14*, 4873–4901.
87. Gunde, M.K.; Kunaver, M.; Čekada, M. Surface analysis of matt powder coatings. *Dye. Pigment.* **2007**, *74*, 202–207.
88. Zhang, J.; Lan, P.; Li, J.; Xu, H.; Wang, Q.; Zhang, X.; Zheng, L.; Lu, Y.; Dai, N.; Song, W. Sol–gel derived near-UV and visible antireflection coatings from hybridized hollow silica nanospheres. *J. Sol-Gel Sci. Technol.* **2014**, *71*, 267–275.
89. Dassanayake, L.S.K.; Kodali, D.R.; Ueno, S.; Sato, K. Physical properties of rice bran wax in bulk and organogels. *J. Am. Oil Chem. Soc.* **2009**, *86*, 1163–1173.
90. Endlein, E.; Peleikis, K.-H. Natural Waxes—Properties, Compositions and Applications. *SÖFW-J.* **2011**, *137*, 16–26.